SCIENCE CHINA
Chemistry

• ARTICLES •

December 2015 Vol.58 No.12: 1884–1890
doi: 10.1007/s11426-015-5390-1

Regulating the mesogenic properties of imidazolium salts by modifying N^3-substituents

Meng Wang[1,2], Xu Pan[2*], Jian Chen[2] & Songyuan Dai[2,3*]

[1]*Anhui Electric Power Design Institute, Hefei 230031, China*
[2]*Key Laboratory of Novel Thin Film Solar Cells, Institute of Plasma Physics, Chinese Academy of Sciences, Hefei 230031, China*
[3]*Beijing Key Laboratory of Novel Thin Film Solar Cells, North China Electric Power University, Beijing 102206, China*

Received January 18, 2015; accepted February 5, 2015; published online May 14, 2015

In this study, a series of imidazolium salts with different N^3-substituents (3-position: methyl, vinyl, ethyl, *n*-propyl, *n*-butyl)-based ionic-liquid crystals with iodide as counterion (ILCs) are synthesized and characterized, with the aim of regulating the mesogenic properties of imidazolium salts. The imidazolium salts-based ionic-liquid crystals are characterized by thermal analysis, polarized optical microscopy, X-ray powder diffraction, and single-crystalline diffraction. Liquid crystalline phase with a Smectic A phase interdigitated bilayer structure is observed. The mesophase temperature range decreases with the increase of the alkyl chain length of N^3-substituent. While when vinyl is attached to the N^3 position, intermolecular π-π interactions are formed in adjacent layers, which exert a positive effect on the formation of mesophase. The layer-spacing of imidazolium salts keeps increasing with the increase of the alkyl chain length attached to both the N^1 and N^3 positions, and gradually decreases with the increasing temperature in liquid crystalline phase. The 1-alkyl-3-vinylimidazolium salt has the smallest layer-spacing, due to the intermolecular π-π interactions between the vinyl and imidazolium rings in adjacent layers.

ionic liquid crystals, mesogenic properties, regulate, N^3-substituents

1 Introduction

Ionic liquid crystals (ILCs) [1], which combine the properties of ionic liquids and liquid crystals, are composed of ionic species and exhibit a mesophase in a certain temperature range. Some of the properties of ILCs differ significantly not only from those of conventional neutral organic liquid crystals, due to their ionic character, but also from conventional ionic liquids because of their anisotropic character caused by their self-organized orientational ordering at the nanometer level [2–5]. They have exhibited interesting potential applications as ion-conductive materials in electrochemical devices [5,6], as organized reaction media for the selectivity for organic reaction [7,8], and as templating agents in materials science [9]. Generally, the mesomorphism can be introduced into such an ionic material by choosing a sufficiently long alkyl chain [10]. The driving forces for the formation of mesophase in such ILCs are thought to be the van der Waals interactions of the alkyl chains, dipole-dipole, cation-π interactions, and π-π stacking, as well as the hydrogen bond between anions and cations [1,11,12]. Therefore, the mesogenic properties of ILCs including the melting point, clearing point, mesophase temperature range, and layer-spacing *d* can be regulated by altering the interactions mentioned above by changing the cations or anions. For instance, ILCs with different cations such as ammonium, phosphonium, pyridinium, and imidazolium salts have been studied [1]. It has been found that with the increase of the long alkyl chain attached to N^1-position, the mesophase temperature range increases drastically. Some groups that have studied counterion effects on mesomorphic properties [7,12–15] have shown that

*Corresponding authors (email: mars_dark@hotmail.com; sydai@ipp.ac.cn)

counterions also greatly affect the mesogenic properties of ILCs.

Because of the widespread use of imidazolium salts-based ionic liquids, many studies have been restricted to 1-alkyl-3-methylimidazolium salts-based ILCs [16–18]. Examples of liquid crystalline 1-alkyl-3-methylimidazolium salts with different counterions such as chloride [19], bromide [20], hexafluorophosphate [16], and tetrafluoroborate [17] have been reported. In most cases, a smectic phase with lamellar structure has been obtained for ILCs. As for 1,3-disubsitituted imidazolium salts, some groups have reported on the mesomorphism of symmetrically substituted 1,3-dialkylibenzimidazolium salts and 1,3-dialkylimidazolium salts-based ILCs [18,21–23]. It has been found that if sufficiently long alkyl chains are attached to both the N^1 and N^3 positions, the imidazolium salts show a mesophase. Luo *et al.* [24] studied 1-alkyl-3-vinyl imidazolium salts-based ILCs and found that the vinyl significantly influences the mesogenic properties of the ILCs. However, to date no systematic studies have been reported about the influence of N^3-substituent on the appearance and structure of the liquid crystalline phase of 1,3-disubstituted imidazolium salts.

Herein, a series of imidazolium salts-based ILCs with iodide as counterion were synthesized and characterized. The imidazolium cations were varied by modifying N^3-substituent (Scheme 1), with the aim of revealing the relationship between the N^3-substituent and the mesogenic properties of imidazolium salts. Imidazolium cations with relatively normal alkyl chains (methyl, ethyl, *n*-propyl, *n*-butyl) and functional group (vinyl) were chosen for their simple structure, with high chemical and electrochemical stability that is preferable for revealing the effects of the N^3-substituent of the imidazolium ring on the mesogenic properties. The physicochemical properties and structures of the obtained imidazolium salts were studied by differential scanning calorimetry (DSC), polarized optical microscopy (POM), small angle X-ray diffraction (SAXD), and single-crystalline diffraction.

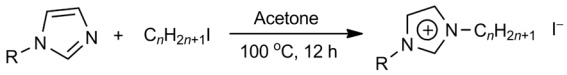

(R=methyl, vinyl, ethyl, *n*-propyl, *n*-butyl)

(*n*=16, 18)

NO.	R (N^3 position)	*n*
1a	methyl	16
1b		18
2a	vinyl	16
2b		18
3a	ethyl	16
3b		18
4a	*n*-propyl	16
4b		18
5a	*n*-butyl	16
5b		18

Scheme 1 Synthesis of imidazolium salts with iodide as counterion.

2 Experimental

2.1 Materials

Diethyl ether and acetone were purchased from Sinopharm Chemical Reagent Co., Ltd. (China). Other reagents were purchased from Acros (USA). All reagents were used as received.

2.2 Synthesis of imidazolium salts

All of the imidazolium salts were synthesized with good yields (>85%, see Supporting Information online) by the quaternization of N-substituted imidazole with corresponding iodide alkane, according to Scheme 1. Take 1-hexadecyl-3-methylimidazolium iodide (**1a**) for example: the mixture of 1-methylimidazole and 1-iodohexadecane was dissolved in acetone. Then the solution was placed into a 58 mL Teflon-lined, stainless-steel autoclave and heated at 100 °C for 12 h. The final product was obtained by multiple crystallizations from diethyl ether. The purity of all the imidazolium salts was confirmed by ^{1}H NMR and elemental analysis (see Supporting Information online).

2.3 Analytical measurements

Differential scanning calorimetry (DSC) was performed with a computer-controlled thermal analyzer (DSC821) with nitrogen as protection gas. The samples were placed in aluminium pans that were cold-sealed under nitrogen. Experimental data are displayed in such a way that exothermic peaks occur at positive heat flow and endothermic peaks at negative heat flow. Heating and cooling rates were 10 K/min. Given temperatures correspond to the onset of the respective thermal process.

Optical observations were made by POM (Olympus BX51, Japan) equipped with a heating stage. Moving images were recorded at a magnification of 100× with a digital camera after the sample was cooled from isotropic phase.

Small-angle X-ray powder diffraction patterns of imidazolium salts were determined using a TTRAX3 diffractometer (Rigaku, Japan) with Cu-Kα X-rays, λ=1.542 Å. Data were recorded in the 2θ ranges of 1°–10° with a step of 0.02° at 293 K. Additionally, X-ray powder diffraction patterns of **3b** at different temperatures were also performed in the 2θ ranges of 2°–7°.

Crystals **2b** were grown by slow evaporation in an acetone solution of **2b**. A few crystals of **2b** were selected at ambient temperature with the help of an optical microscope. The selected crystals were mounted on a Nonius Kappa-CCD area-detector diffractometer (Cu-Kα, λ=1.542 Å). Cell parameters were determined from reflections recorded

in 10 frames (1.0° in ϕ, 20 s). The crystal structures were solved by direct methods using SHELXS-97 [25] and expanded using difference Fourier techniques, refined by SHELXL-97 [26] and full-matrix least-squares calculations. All H atoms attached to C atoms were positioned geometrically with C–H=0.93, 0.97, and 0.96 Å. Further details of the data collections and structure refinements are given in Supporting Information online. CCDC-815835 contain(s) the supplementary crystallographic data for this paper. These data can be obtained free of charge from the Cambridge Crystallographic Data Centre (www.ccdc.cam.ac.uk/data_request/cif).

3 Results and discussion

3.1 Thermal properties of ILCs

The DSC data (phase-transition temperatures and phase-transition enthalpies, ΔH) are listed in Table 1 (Figure S2). For **1a–3b**, a mesophase is obvious in both the heating and cooling processes. When the *n*-propyl is attached to N^3 position, only **4b** displays a relatively lower mesophase-temperature range. For the imidazolium salts with *n*-butyl attached to the N^3 position (**5a**, **5b**), no mesophase is observed in the detected temperature range. This phenomenon indicates that the N^3-substituent of the imidazolium ring influences the formation of mesophase drastically.

Table 1 Summary of the DSC analysis for imidazolium salts **1a–5b**, including the heating and cooling processes

NO.	Phase transition [a]	Heating		Cooling	
		T (°C)	ΔH (kJ/mol)	T (°C)	ΔH (kJ/mol)
1a	Cryst1 [b]-Cryst	49.85	7.15	–	–
	Cryst-SmA	65.1	40.69	38.9	–27.21
	SmA-Iso	187.5	1.15	184.9	–1.16
1b	Cryst2–Cryst1	56.5	12.00	4.3	–0.10
	Cryst1-Cryst	62.2	2.48	37.0	–0.21
	Cryst-SmA	72.2	26.91	51.5	–36.25
	SmA-Iso	218.5	1.34	192.6	–1.24
2a	Cryst-SmA	69.9	81.08	37.3	–34.65
	SmA-Iso	145.5	1.07	143.6	–1.08
2b	Cryst-SmA	76.1	88.26	51.4	–43.09
	SmA-Iso	184.9	1.40	182.9	–1.33
3a	Cryst-SmA	63.7	64.06	38.9	–32.40
	SmA-Iso	103.4	0.67	102.7	–0.68
3b	Cryst-SmA	71.2	75.90	52.8	–43.16
	SmA-Iso	147.8	1.07	147.2	–1.05
4a	Cryst-Iso	52.4	58.81	32.9	–35.85
4b	Cryst-SmA	60.9	69.24	48.3	–43.59
	SmA-Iso	76.0	0.41	75.6	–0.40
5a	Crst1-Crst	23.6	0.95	–	–
	Cryst-I	48.6	55.88	24.9	–40.32
5b	Cryst-I	60.2	66.93	42.5	–46.32

a) The symbols cryst, iso, and SmA denote crytstal, isotropic liquid, and A liquid crystal with a Smectic A phase; b) Cryst1 and Cryst2 denote the different structure in crystalline phase probably caused by the comformational change of molecules.

Figure 1 summarizes the mesogenic behavior of the imidazolium salts-based ILCs during the heating process. From Figure 1, it can be seen that the melting point does not vary significantly for the imidazolium salts with the same *n* values, which suggests that the melting point mainly depends on the anion. By contrast, the clearing point varies significantly and follows the order of methyl>vinyl>ethyl> *n*-propyl, which indicates that the increasing alkyl chain length of the N^3-substitutent exerts a negative effect on the formation of mesophase. The vinyl attached to the N^3 position would benefit the mesophase stability more than ethyl.

As reported [27], the ethyl, *n*-propyl, and *n*-butyl are more flexible than the rigid methyl and planar vinyl. From these results, we inferred that with the increase of the alkyl length attached to the N^3 position, the intermolecular π-π stacking and hydrogen bond between the iodide and the proton of the aromatic ring would decrease, which in turn would drastically lower the clearing point. Typically for the imidazolium salts with *n*-propyl attached to the N^3 position, when *n*=16 (**4a**), no mesophase is observed due to the existence of flexible *n*-propyl. When *n*=18 (**4b**), a relatively low mesophase temperature range is obtained due to the increase of the positive van der Waals interactions caused by the increasing length of the long alkyl chain attached to the N^1 position. When *n*-butyl is attached to the N^3 position, no mesophase is obtained in either **5a** or **5b**. Thus, on the one hand, the mesophase stability of imidazolium salts increases with the increase of the length of the alkyl chain attached to the N^1 position; on the other hand, it decreases with the increase of the length of the alkyl chain attached to the N^3 position. As for **2a** and **2b**, the intermolecular π-π stacking interactions are formed between vinyl and imidazolium rings, which exert a positive effect on the formation of mesophase. These details will be discussed in a subsequent section.

It is also noteworthy that in the heating and cooling processes, the ΔH of the imidazolium salts with the same *n* value on the clearing point follows the order of methyl>

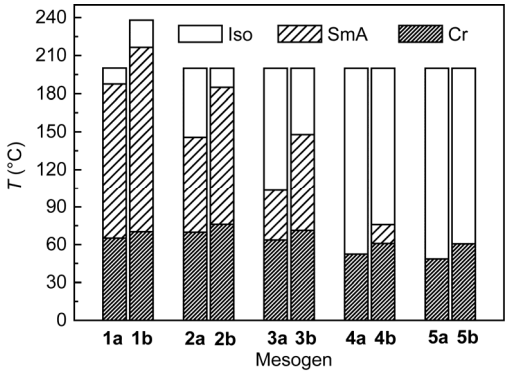

Figure 1 Mesogenic behavior of imidazolium salts **1a–5b** during the heating process.

vinyl>ethyl>propyl (Table 1 and Figure S3), which is mainly associated with the stability of mesophase (in fact, these are the driving forces for the formation of liquid crystalline phase). As they cool, all of the samples show larger temperature ranges for mesophase than during the heating process, due to the extensive supercooling before crystallisation that is typical for the imidazolium salts [17].

3.2 Structural properties

The presence of the mesophase is also supported by the textures observed through a polarized optical microscope (POM) (Figure S4). Figure 2 shows a POM texture of **2b** that is typical of the imidazolium salts-based ILCs presented here. The obviously focal conic fan textures with large dark homeotropic areas confirm their layered structure. These results suggest that the liquid crystalline mesophase can be assigned to Smectic A mesophase (SmA), a result that has also been observed for other 1-alkyl-3-methylimidazolium ILCs [19]. Therefore, a lamellar mesophase of SmA with an average direction perpendicular to the layer surface is proposed. This identification is also supported by the small-angle XRD data described below, and by the confirmation of mesophase as an interdigital bilayer SmA phase [12].

First, SAXD patterns are performed at the crystalline phase in the low-angle region ($0<2\theta<10°$) (Figure S5). Sharp peaks observed in the low-angle region indicate the formation of layered structures [28]. Figure 3 shows layer-spacing d of imidazolium salts at crystalline phase (Table S1). It is obvious that for the imidazolium salts with the same N^3-substituent, the layer-spacing d keeps increasing with the increasing n values, an effect similar to other ILCs [29,30]. More important, for the imidazolium salts with the same n values, the layer-spacing d follows the sequence vinyl<methyl<ethyl<*n*-propyl<*n*-butyl. Even in the liquid crystalline mesophase, we may infer that the layer-spacing d follows the same order [12,28]. The layer-spacing d (except for **2a** and **2b**) is found to satisfy $l<d<2l$, where l is the fully extended length of the cation and is roughly estimated from crystallographic data [31]. This result suggests that an interdigitated bilayer structure is formed in SmA mesophase [32]. Moreover, in an interesting phenomenon, the layer-spacings d of **2a** and **2b** are the smallest—even lower than the fully extended length of the cation in crystalline phase. It is likely that the alkyl chain of the cation is tilted with respect to the layer plane with a large tilt angle in crystalline phase. This means that the vinyl plays a crucial role on the unique properties of **2a** and **2b**, which is different from other alkyl substituents attached to the N^3 position.

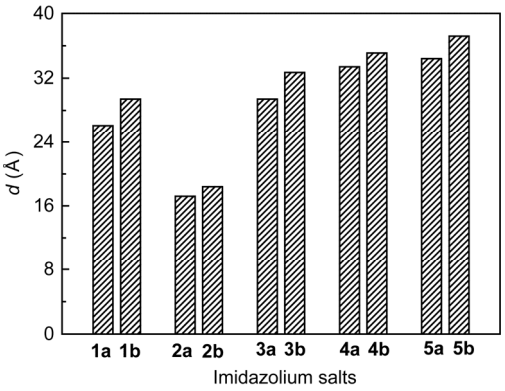

Figure 3 Layer-spacing d of imidazolium salts **1a**–**5b** in crystalline phase (293 K).

The SAXD patterns of **3b** (Figure 4) are performed at different temperatures to study the structural transformation of imidazolium salts with phase transition. For **3b**, peaks in crystalline are sharper than in liquid crystalline mesophase and only one peak is shown in liquid crystalline phase, which suggests the loss of positional ordering in the layer plane in liquid crystalline phase due to the melting of the long alkyl chain [12]. It is noteworthy that the shift of the main peak in the crystalline phase is negligible, whereas the peak in the liquid crystalline phase shifts to the high angle with increasing temperature. Figure 5 shows the dependence of layer-spacing d on temperature. In crystalline phase, layer-spacing d does not change with the increase of temperature and in liquid crystalline phase it gradually decreases with increasing temperature. Additionally, the layer-spacing d is

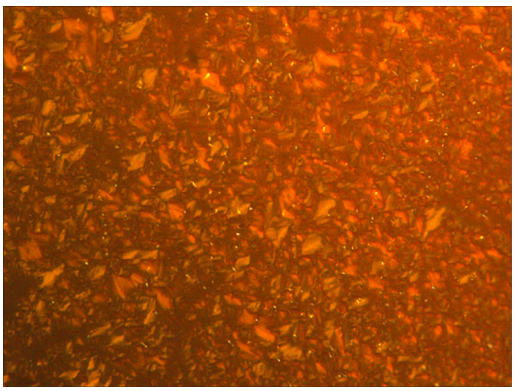

Figure 2 Polarized optical microscopic textures of **2b** at 160 °C.

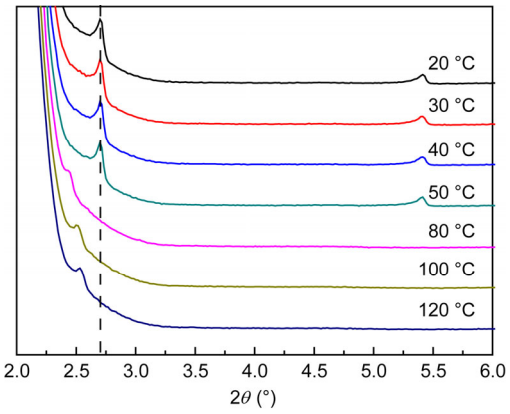

Figure 4 SAXD patterns of **3b** at different temperatures.

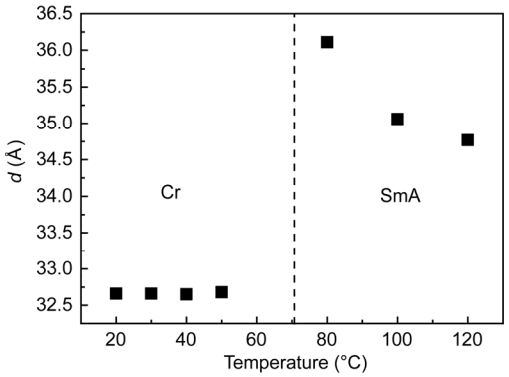

Figure 5 Dependence of layer-spacing *d* of **3b** on temperature.

smaller in crystalline phase than in liquid crystalline phase, which indicates that the alkyl chain of the cation is also tilted to the layer plane in crystalline phase (Figure 6). When phase transition from crystalline to mesophase occurs, the tilted angle of the layer structure decreases with increasing temperature, leading to an increase of the layer-spacing *d*. Whereas in SmA phase, the bilayer structure interdigitates more deeply with increasing temperature due to the increase of thermal mobility of the long alkyl chains, leading to a decrease of the layer-spacing (Figure 6).

3.3 Crystal structure of 1-octadecyl-3-vinyl imidazolium iodide (2b)

As mentioned above, the N^3-substituent exerted a significant effect on the formation of the mesophase and structural property of the imidazolium salts. Therefore, to elucidate this formation in detail, single-crystal X-ray diffraction is needed. However, to date we were unable to produce crystals of most salts with a quality sufficient for a full structure determination, due to the formation of very thin platelike crystals. Only **2b** (1-octadecyl-3-vinylimidazolium iodide) showed sufficient quality for single-crystalline X-ray diffraction, which indicated that the exocyclic conjugated double bond would benefit the crystal growth. Nonetheless, we can qualitatively illuminate the role of N^3-substituent on the formation of mesophase and the structural property of imidazolium salts.

As seen in Figure 7(a, b), the crystal structure of **2b** consists of a discrete cation and anion. The imidazolium ring with vinyl attached to the N^3-position is completely planar. Selected geometric parameters are shown in Table 2. The relatively short bond length of N1–C4 (compared to N2–C6) indicates that the π electrons of the vinyl and the imidazolium ring are delocalized. The straight alkyl chain is disrupted close to the imidazolium ring, where it adopts a bent conformation as shown by the respective torsion angles C2–N2–C6–C7, C3–N2–C6–C7, N2–C6–C7–C8, and C6–C7–C8–C9, which are –158.9(3)°, 26.5(7)°, 170.6(3)°, and 175.0(3)°. All other carbon-chain torsion angles approach 180°. Thus, the cation has a spoon-shaped structure. The crystal structure of **2b** consists of sheet imidazolium rings and iodide ions separated by interdigitated alkyl chains. Of note is the lamellar structure with a long alkyl chain that is tilted relative to the layers of cations (about 45° from the normal of the layer plane (*a*-*b* plane), which can explain the smallest layer-spacing of *d* (*l* is about 26.3 Å, estimated from crystallographic data). The layer-spacing *d* is 18.76 Å obtained from single-crystal data, which is equivalent to the spacing calculated from powder XRD data for **2b** (18.4 Å) within the margin of experimental error (Figure 7(c)).

As reported, single-crystalline technique can be used to characterize the hydrogen bond, including bond length and bond angle [20]. Luo's study [24] also showed that the vinyl

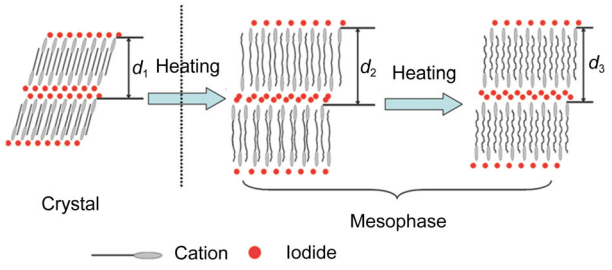

Figure 6 Schematic of melting of bilayer structure from crystalline phase to mesophase (d_1<d_3<d_2).

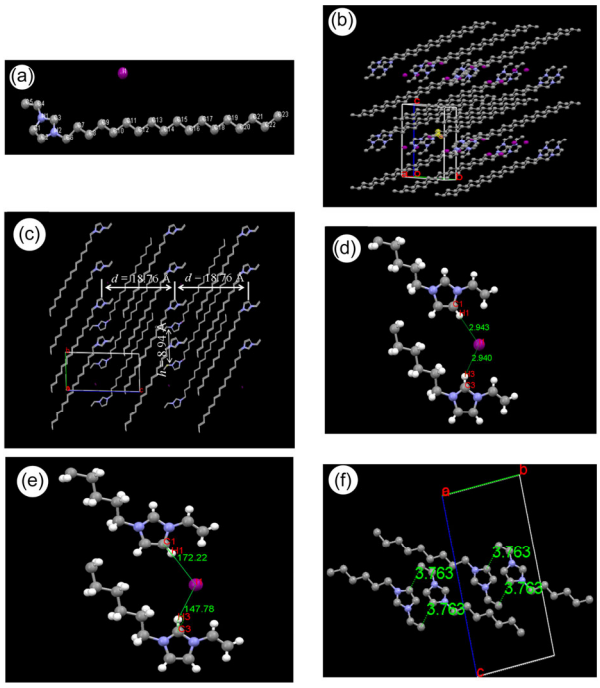

Figure 7 (a) X-ray structure of **2b** in the solid state (the numbering of atoms given here are used only for the X-ray diffraction studies); (b) unit cell of **2b**; (c) partial crystal packing of **2b** projected on the (*b*-*c*) plane; (d) H-bond between iodide and hydrogen of imidazolium ring in **2b** (Å): H1···I1 2.943, H3···I1 2.940; (e) angles of H-bond in **2b** (°): ∠I1···H1–C1 172.2, ∠I1···H3–C3 147.78; (f) intermolecular π-π stacking between imidazolium rings of different layers in **2b**. Some atoms are omitted.

Table 2 Selected interatomic distances and torsion angles

Bond	Distance (Å)	Bond	Torsion angles (°)
N1–C3	1.333(4)	C2–N2–C6–C7	–158.9(3)
N1–C4	1.422(4)	N2–C6–C7–C8	175.0(3)
N1–C1	1.378(4)	C3–N2–C6–C7	26.5(7)
N2–C3	1.311(4)	C6–C7–C8–C9	170.6(3)
C4–C5	1.295(5)		
C2–C1	1.332(5)		
N2–C6	1.479(4)		

functionalization provides additional hydrogen bonding interactions between the cations and anions. Therefore, from the crystallographic data it is reasonable to infer that the iodide anion forms two hydrogen bonds with two different imidazolium cations in the same layer (Figure 7(d, e)): one at ring C3–H with a bond length of 2.940 Å (H3···I1) and an angle of 147.8°, and the other at ring C1–H with a bond length of 2.943 Å (H1···I1) and an angle of 172.2°. It is also noteworthy that there are intermolecular π-π stacking interactions between the vinyl and the imidazolium rings at an average distance of 3.763 Å in adjacent layers (Figure 7(f)). This result can explain the relatively large mesophase temperature range.

According to previous reports, the hydrogen bond between anion and protons of imidazolium ring will exert great effects on the properties of imidazolium salts [1,12,33,34]. Generally, the ethyl, *n*-propyl, and *n*-butyl substituents are more flexible than the rigid vinyl and methyl due to their complicated conformation caused by the rotation of the C–C and C–N bonds. Therefore, once they are attached to the N^3 position, the hydrogen bond would drastically weaken due to their steric hindrance effect between the anion and protons of the imidazolium cation. In addition, intermolecular π-π stacking interactions would be impossible. Thus, the mesophase stability of imidazolium salts follows the sequence vinyl>ethyl>*n*-propyl>*n*-butyl. However, the volume of $–CH=CH_2$ is larger than that of $–CH_3$; in addition, it weakens the hydrogen bond between the anion and the proton of the aromatic ring due to steric hindrance, which could not be offset by the π-π stacking interactions. Therefore, compared with $–CH_3$, $–CH=CH_2$ attached to the N^3 position exerts a negative effect on the formation of mesophase. This result indicates that the hydrogen bond has a more positive effect than π-π stacking interactions on the formation of mesophase. Moreover, if the alkyl chain length of the N^3-substituents continues to increase, mesophase may be observed due to the increasing van der Waals interactions [21]. In short, different N^3-substituents of imidazolium rings would result in different effects on the driving forces for the formation of mesophase, and consequently on the mesogenic properties. Thus, we can regulate the mesogenic properties of imidazolium salts-based ILCs as necesary by introducing different substituents or functional groups to the N^3 position on the imidazolium ring.

4 Conclusions

A series of imidazolium salts with different N^3-substituents (methyl, vinyl, ethyl, *n*-propyl, and *n*-butyl)-based ILCs are synthesized and their mesogenic properties, including melting point, clearing point, and structural properties, are characterized. By introducing different substituents to the N^3 position of the imidazolium ring, the mesogenic properties of ILCs are successfully regulated. The increasing alkyl chain length of the N^3-substituent exerted negative effect on the formation and stability of the SmA phase, which is associated with the weakening of the hydrogen bond between iodide and the protons of the imidazolium ring due to their increasing steric hindrance effects. The layer-spacing *d* also keeps increasing with the increasing length of the alkyl chain attached to the N^3 position. For the imidazolium salts with vinyl attached to the N^3 position, extensive π-π stacking interactions between the vinyl and the imidazolium ring in adjacent layers are formed, which results in a relatively large temperature range for mesophase. In addition, these adjacent layers tilt the alkyl chain of the cation with respect to the layer plane in the crystalline phase, which results in smallest layer-spacing *d*. These results suggest that the mesogenic properties of imidazolium salts-based ILCs can be regulated by the modification of the N^3 substituents of the imidazolium ring. Further regulation of the driving forces for the formation of mesophase by changing the anion will be pursued.

Supporting information

The supporting information is available online at chem.scichina.com and link.springer.com/journal/11426. The supporting materials are published as submitted, without typesetting or editing. The responsibility for scientific accuracy and content remains entirely with the authors.

This work was financially supported by the National Basic Research Program of China (2011CBA00700), the National Natural Science Foundation of China (21103197, 21273242), and China Postdoctoral Science Foundation (2013M540526).

1 Binnemans K. Ionic liquid crystals. *Chem Rev*, 2005, 105: 4148–4204
2 Trilla M, Pleixats R, Parella T, Blanc C, Dieudonne P, Guari Y, Man MWC. Ionic liquid crystals based on mesitylene-containing bis- and trisimidazolium salts. *Langmuir*, 2008, 24: 259–265
3 Yoshio M, Mukai T, Kanie K, Yoshizawa M, Ohno H, Kato T. Layered ionic liquids: anisotropic ion conduction in new self-organized liquid-crystalline materials. *Adv Mater*, 2002, 14: 351–354
4 Yoshio M, Mukai T, Kanie K, Yoshizawa M, Ohno H, Kato T. Liquid-crystalline assemblies containing ionic liquids: an approach to anisotropic ionic materials. *Chem Lett*, 2002: 320–321
5 Yamanaka N, Kawano R, Kubo W, Masaki N, Kitamura T, Wada Y, Watanabe M, Yanagida S. Dye-sensitized TiO_2 solar cells using imidazolium-type ionic liquid crystal systems as effective electrolytes. *J Phys Chem B*, 2007, 111: 4763–4769
6 Pan X, Wang M, Fang XQ, Zhang CN, Huo ZP, Dai SY. Ionic liquid

crystal-based electrolyte with enhanced charge transport for dye-sensitized solar cells. *Sci China Chem*, 2013, 56: 1463–1469
7 Lee CK, Huang HW, Lin IJB. Simple amphiphilic liquid crystalline *N*-alkylimidazolium salts. A new solvent system providing a partially ordered environment. *Chem Commun*, 2000: 1911–1912
8 Weiss RG. Liquid-crystalline solvents as mechanistics probes .30. Thermotropic liquid-crystals as reaction media for mechanistic investigations. *Tetrahedron*, 1988, 44: 3413–3475
9 Faul CFJ, Antonietti M. Ionic self-assembly: facile synthesis of supramolecular materials. *Adv Mater*, 2003, 15: 673–683
10 Bruce DW, Metrangolo P, Meyer F, Prasang C, Resnati G, Terraneo G, Whitwood AC. Mesogenic, trimeric, halogen-bonded complexes from alkoxystilbazoles and 1,4-diiodotetrafluorobenzene. *New J Chem*, 2008, 32: 477–482
11 Bonhote P, Dias AP, Papageorgiou N, Kalyanasundaram K, Grätzel M. Hydrophobic, highly conductive ambient-temperature molten salts. *Inorg Chem*, 1996, 35: 1168–1178
12 Bradley AE, Hardacre C, Holbrey JD, Johnston S, McMath SEJ, Nieuwenhuyzen M. Small-angle X-ray scattering studies of liquid crystalline 1-alkyl-3-methylimidazolium salts. *Chem Mater*, 2002, 14: 629–635
13 Martin BS, Elena K, Hans-Ullrich S, Birgit C, Peter Fischer WF, Sabine L. Influence of *N*-alkyl substituents and counterions on the structural and mesomorphic properties of guanidinium salts: experiment and quantum chemical calculations. *ChemPhysChem*, 2010, 11: 3752–3765
14 Zhang QX, Jiao LS, Shan CS, Hou P, Chen B, Xu XY, Niu L. Synthesis and characterisation of novel imidazolium-based ionic liquid crystals with a *p*-nitroazobenzene moiety. *Liq Cryst*, 2008, 35: 765–772
15 Dobbs W, Douce L, Allouche L, Louati A, Malbosc F, Welter R. New ionic liquid crystals based on imidazolium salts. *New J Chem*, 2006, 30: 528–532
16 Gordon CM, Holbrey JD, Kennedy AR, Seddon KR. Ionic liquid crystals: hexafluorophosphate salts. *J Mater Chem*, 1998, 8: 2627–2636
17 Holbrey JD, Seddon KR. The phase behaviour of 1-alkyl-3-methylimidazolium tetrafluoroborates; ionic liquids and ionic liquid crystals. *J Chem Soc Dalton Trans*, 1999: 2133–2139
18 Reichert WM, Holbrey JD, Swatloski RP, Gutowski KE, Visser AE, Nieuwenhuyzen M, Seddon KR, Rogers RD. Solid-state analysis of low-melting 1,3-dialkylimidazolium hexafluorophosphate salts (ionic liquids) by combined X-ray crystallographic and computational analyses. *Cryst Growth Design*, 2007, 7: 1106–1114
19 Bowlas CJ, Bruce DW, Seddon KR. Liquid-crystalline ionic liquids. *Chem Commun*, 1996: 1625–1626
20 Getsis A, Mudring AV. Imidazolium based ionic liquid crystals: structure, photophysical and thermal behaviour of [$C_n$mim]Br center dot $x$$H_2O$ (n=12, 14; x=0, 1). *Cryst Res Technol*, 2008, 43: 1187–1196
21 Lee KM, Lee CK, Lin IJB. First example of interdigitated U-shape benzimidazolium ionic liquid crystals. *Chem Commun*, 1997: 899–900
22 Lee CK, Peng HH, Lin IJB. Liquid crystals of *N*,*N*′-dialkylimidazolium salts comprising palladium(II) and copper(II) ions. *Chem Mater*, 2004, 16: 530–536
23 Wang XJ, Heinemann FW, Yang M, Melcher BU, Fekete M, Mudring AV, Wasserscheid P, Meyer K. A new class of double alkyl-substituted, liquid crystalline imidazolium ionic liquids: a unique combination of structural features, viscosity effects, and thermal properties. *Chem Commun*, 2009: 7405–7407
24 Luo SC, Sun SW, Deorukhkar AR, Lu JT, Bhattacharyya A, Lin IJB. Ionic liquids and ionic liquid crystals of vinyl functionalized imidazolium salts. *J Mater Chem*, 2011, 21: 1866–1873
25 Sheldrick GM. SHELXS-97. Program for X-ray crystal structure refinement. Gottingen: University of Gottingen, 1997
26 Sheldrick GM. SHELXL-97. Program for X-ray crystal structure solution. Gottingen: University of Gottingen, 1997
27 Fei Z, Kuang D, Zhao D, Klein C, Ang WH, Zakeeruddin SM, Grätzel M, Dyson PJ. A Supercooled imidazolium iodide ionic liquid as a low-viscosity electrolyte for dye-sensitized solar cells. *Inorg Chem*, 2006, 45: 10407–10409
28 Xu F, Matsumoto K, Hagiwara R. Effects of alkyl chain length on properties of 1-alkyl-3-methylimidazolium fluorohydrogenate ionic liquid crystals. *Chem Euro J*, 2010, 16: 12970–12976
29 De Roche J, Gordon CM, Imrie CT, Ingram MD, Kennedy AR, Lo Celso F, Triolo A. Application of complementary experimental techniques to characterization of the phase behavior of [C_{16}mim][PF_6] and [C_{14}mim][PF_6]. *Chem Mater*, 2003, 15: 3089–3097
30 Lava K, Binnemans K, Cardinaels T. Piperidinium, piperazinium and morpholinium ionic liquid crystals. *J Phys Chem B*, 2009, 113: 9506–9511
31 Goossens K, Nockemann P, Driesen K, Goderis B, Gorller-Walrand C, Van Hecke K, Van Meervelt L, Pouzet E, Binnemans K, Cardinaels T. Imidazolium ionic liquid crystals with pendant mesogenic groups. *Chem Mater*, 2008, 20: 157–168
32 Li LB, Groenewold J, Picken SJ. Transient phase-induced nucleation in ionic liquid crystals and size-frustrated thickening. *Chem Mater*, 2005, 17: 250–257
33 Elaiwi A, Hitchcock PB, Seddon KR, Srinivasan N, Tan YM, Welton T, Zora JA. Hydrogen-bonding in imidazolium salts and its implications for ambient-temperature halogenoaluminate(III) ionic liquids. *J Chem Soc Dalton Trans*, 1995: 3467–3472
34 Hunt PA. Why does a reduction in hydrogen bonding lead to an increase in viscosity for the 1-butyl-2,3-dimethyl-imidazolium-based ionic liquids? *J Phys Chem B*, 2007, 111: 4844–4853